JNeurosci
THE JOURNAL OF NEUROSCIENCE

Research Articles: Behavioral/Cognitive

Subthalamic nucleus and sensorimotor cortex activity during speech production

A Chrabaszcz[1], WJ Neumann[2], O Stretcu[3], WJ Lipski[4], A Bush[4,5], C Dastolfo-Hromack[4], D Wang[4,6], DJ Crammond[4], S Shaiman[7], MW Dickey[7], LI Holt[8], RS Turner[9,10], JA Fiez[1,7,10] and RM Richardson[4,9,10]

[1]*Department of Psychology, University of Pittsburgh, 15213*
[2]*Movement Disorder and Neuromodulation Unit, Department of Neurology, Campus Mitte, Charité—Universitätsmedizin Berlin, Berlin, Germany, 10117*
[3]*Machine Learning Department, School of Computer Science, Carnegie Mellon University, 15213*
[4]*Brain Modulation Lab, Department of Neurological Surgery, University of Pittsburgh School of Medicine, 15213*
[5]*Department of Physics, FCEN, University of Buenos Aires and IFIBA-CONICET, Argentina, 1428*
[6]*School of Medicine, Tsinghua University, Beijing, China 100084*
[7]*Department of Communication Science and Disorders, University of Pittsburgh, 15213*
[8]*Department of Psychology, Carnegie Mellon University, 15213*
[9]*Department of Neurobiology, University of Pittsburgh School of Medicine, 15213*
[10]*University of Pittsburgh Brain Institute, 15213*

https://doi.org/10.1523/JNEUROSCI.2842-18.2019

Received: 5 November 2018

Revised: 11 January 2019

Accepted: 18 January 2019

Published: 30 January 2019

Author contributions: A.C., W.L., C.A.D.-H., S.S., M.D., L.H., R.S.T., J.A.F., and R.M.R. designed research; A.C., W.L., C.A.D.-H., D.J.C., and R.M.R. performed research; A.C., W.-J.N., O.S., W.L., A.B., D.W., J.A.F., and R.M.R. analyzed data; A.C. wrote the first draft of the paper; A.C., W.-J.N., O.S., W.L., A.B., C.A.D.-H., D.W., D.J.C., S.S., M.D., L.H., R.S.T., J.A.F., and R.M.R. edited the paper; A.C. wrote the paper.

Conflict of Interest: The authors declare no competing financial interests

Funding was provided by NINDS U01NS098969 (PI: Richardson), the Hamot Health Foundation (PI: Richardson), and a University of Pittsburgh Brain Institute NeuroDiscovery Pilot Research Award (PI: Richardson). The authors are thankful to the patients who participated in this study and the clinical staff who facilitated data collection.

Correspondence should be addressed to To whom correspondence should be addressed: Mark Richardson, MD, PhD, richardsonrm@upmc.edu, Department of Neurological Surgery, University of Pittsburgh Medical Center, 200 Lothrop St., Suite B400, Pittsburgh, PA 15213

Cite as: J. Neurosci 2019; 10.1523/JNEUROSCI.2842-18.2019

Subthalamic nucleus and sensorimotor cortex activity during speech production

Abbreviated title: Subthalamic and cortical activity during speech

Chrabaszcz A[1], Neumann WJ[2], Stretcu O[3], Lipski WJ[4], Bush A[4,5], Dastolfo-Hromack C[4], Wang D[4,6], Crammond DJ[4], Shaiman S[7], Dickey MW[7], Holt LL[8], Turner RS[9,10], Fiez JA[1,7,10], *Richardson RM[4,9,10]

[1]Department of Psychology, University of Pittsburgh, 15213; [2]Movement Disorder and Neuromodulation Unit, Department of Neurology, Campus Mitte, Charité – Universitätsmedizin Berlin, Berlin, Germany, 10117; [3]Machine Learning Department, School of Computer Science, Carnegie Mellon University, 15213; [4]Brain Modulation Lab, Department of Neurological Surgery, University of Pittsburgh School of Medicine, 15213; [5]Department of Physics, FCEN, University of Buenos Aires and IFIBA-CONICET, Argentina, 1428; [6]School of Medicine, Tsinghua University, Beijing, China 100084; [7]Department of Communication Science and Disorders, University of Pittsburgh, 15213; [8]Department of Psychology, Carnegie Mellon University, 15213; [9]Department of Neurobiology, University of Pittsburgh School of Medicine, 15213; [10]University of Pittsburgh Brain Institute, 15213

*To whom correspondence should be addressed:

Mark Richardson, MD, PhD
richardsonrm@upmc.edu
Department of Neurological Surgery, University of Pittsburgh Medical Center
200 Lothrop St., Suite B400, Pittsburgh, PA 15213

Number of pages: 35

Number of figures: 5 Number of tables: 2

Number of words in Abstract: 249 Introduction: 644 Discussion: 1534

Conflict of Interest: The authors declare no competing financial interests

Acknowledgements: Funding was provided by NINDS U01NS098969 (PI: Richardson), the Hamot Health Foundation (PI: Richardson), and a University of Pittsburgh Brain Institute NeuroDiscovery Pilot Research Award (PI: Richardson). The authors are thankful to the patients who participated in this study and the clinical staff who facilitated data collection.

ABSTRACT

The sensorimotor cortex is somatotopically organized to represent the vocal tract articulators, such as lips, tongue, larynx, and jaw. How speech and articulatory features are encoded at the subcortical level, however, remains largely unknown. We analyzed local field potential (LFP) recordings from the subthalamic nucleus (STN) and simultaneous electrocorticography recordings from the sensorimotor cortex of 11 human subjects (1 female) with Parkinson's disease during implantation of deep brain stimulation (DBS) electrodes, while they read aloud three-phoneme words. The initial phonemes involved either articulation primarily with the tongue (coronal consonants) or the lips (labial consonants). We observed significant increases in high gamma (60–150 Hz) power in both the STN and the sensorimotor cortex that began before speech onset and persisted for the duration of speech articulation. As expected from previous reports, in the sensorimotor cortex, the primary articulators involved in the production of the initial consonants were topographically represented by high gamma activity. We found that STN high gamma activity also demonstrated specificity for the primary articulator, although no clear topography was observed. In general, subthalamic high gamma activity varied along the ventral-dorsal trajectory of the electrodes, with greater high gamma power recorded in the dorsal locations of the STN. Interestingly, the majority of significant articulator-discriminative activity in the STN occurred prior to that in sensorimotor cortex. These results demonstrate that articulator-specific speech information is contained within high gamma activity of the STN, but with different spatial and temporal organization compared to similar information encoded in the sensorimotor cortex.

Key words: speech, vocal tract articulators, subthalamic nucleus, sensorimotor cortex, high gamma oscillations, electrocorticography, deep brain stimulation, Parkinson's disease

SIGNIFICANCE STATEMENT

Clinical and electrophysiological evidence suggest that the subthalamic nucleus is involved in speech, however, this important basal ganglia node is ignored in current models of speech production. We previously showed that subthalamic nucleus neurons differentially encode early and late aspects of speech production, but no previous studies have examined subthalamic functional organization for speech articulators. Using simultaneous local field potential recordings from the sensorimotor cortex and the subthalamic nucleus in patients with Parkinson's disease undergoing deep brain stimulation surgery, we discovered that subthalamic nucleus high gamma activity tracks speech production at the level of vocal tract articulators, prior to the onset of vocalization and often prior to related cortical encoding.

INTRODUCTION

Speech articulation constitutes a complex motor behavior involving a precise coordination of different parts of the vocal apparatus, known as articulators (e.g., lips, tongue). While recruitment of the cortical regions in the articulatory realization of speech is widely documented, the specific contributions of different subcortical structures remain largely unknown. Here, for the first time, we use local field potential (LFP) recordings from the subthalamic nucleus (STN) and simultaneous electrocorticography (ECoG) recordings from the sensorimotor cortex to investigate the role of the STN in speech articulation and to compare its spatial and temporal organization for encoding of speech articulators with that of the sensorimotor cortex.

Ample evidence has implicated the ventral-lateral orofacial area of the sensorimotor cortex as a principal cortical region for the neural representation of speech articulators. Electrical stimulation of this region produces somatotopically organized sensorimotor responses for the larynx, tongue, jaw, and lips along the ventral-to-dorsal orientation of the central sulcus, respectively (Penfield and Boldrey, 1937; Penfield, 1954; Woolsey, Erickson, and Gilson, 1979; Breshears, Molinaro, and Chang, 2015). Functional imaging (fMRI) studies generally provide corroborating evidence for the somatotopic cortical representation of the vocal tract effectors, among other body parts, albeit with a varying degree of overlap among individuals (Lotze et al., 2000; Hesselmann et al., 2004; Pulvermüller et al., 2006; Brown, Ngan, and Liotti, 2007; Meier et al., 2008; Takai, Brown, and Liotti, 2010; Carey et al., 2017). Recently, ECoG studies have elaborated the notion of cortical articulatory somatotopy by revealing differentiated neural representations for fine-grained phonetic features and complex kinematics underlying speech articulation (Bouchard et al., 2013; Bouchard & Chang, 2014; Mugler et al., 2014; Lotte et al., 2015; Bouchard et al., 2016; Cheung et al., 2016; Ramsey et al., 2017; Chartier et al., 2018; Conant et al., 2018).

Anatomical connections between the sensorimotor cortex and the basal ganglia via a cortico-striatal-thalamic loop (Alexander, DeLong, and Strick, 1986) suggest that the basal ganglia, including the STN, may also participate in speech production. Indeed, indirect evidence from lesion literature (Brunner et al., 1982; Damasio et al., 1982; Wallesch et al., 1983; Nadeau and Crosson, 1997), from clinical data on deep brain stimulation (DBS) outcomes (Morrison et al., 2004; Witt et al., 2008; Aldridge et al., 2016; Knowles et al., 2018) and neurological disorders involving the basal ganglia (Logemann et al., 1978; Ho et al., 1998; Walsh and Smith, 2012) implicates the basal ganglia in many aspects of speech production. Direct evidence from electrophysiological recordings of STN activity during speech production shows decrease in beta power during articulation of non-propositional speech (Hebb, Darvas, and Miller, 2012), and speech-related changes in single unit firing activity (Watson and Montgomery, 2006; Lipski et al., 2018). To our knowledge, however, no study has investigated the spatial and temporal distribution of speech-related neuronal activity for different articulators in the STN relative to the sensorimotor cortex. Given that the STN is anatomically subdivided into sensorimotor, limbic, and associative functional areas (Hamani et al., 2004; Temel et al., 2005; Haynes and Haber, 2013) and that a somatotopic organization for arms, legs, eyes and face is observed within the motor territory of the STN in human and non-human primates (Monakow, Akert, and Kiinzle, 1978; DeLong, Crutcher, and Georgopoulos, 1985; Wichmann, Bergman, and DeLong, 1994; Rodriguez-Oroz et al., 2001; Starr, Theodosopoulos, and Turner, 2003; Theodosopoulos et al., 2003; Nambu, 2011), it is possible that a functional somatotopy for the vocal tract articulators is also maintained within the STN.

We employed a novel experimental paradigm in awake, speaking patients undergoing STN-DBS for Parkinson's disease, where sensorimotor electrocorticography is recorded simultaneously with STN LFPs. We discovered that STN high gamma (60–150 Hz) activity is dynamic during the production of speech, exhibiting activity that tracks with specific articulatory

motor features. Our data further suggest that spatial and temporal characteristics of the neural representations of speech articulators may differ between the cortex and STN.

MATERIALS AND METHODS

Participants. Participants included 11 native English-speaking patients with Parkinson's disease (10M/1F, age: 67.5±7.7 years, duration of disease: 8±2.4 years) undergoing awake stereotactic neurosurgery for implantation of DBS electrodes in the STN. In addition to the clinical subcortical mapping and as part of an IRB approved research protocol, participants were temporarily implanted with subdural electrode arrays over the left ventral sensorimotor cortex. All patients completed Unified Parkinson's Disease Rating Scale (UPDRS) testing within four months before the surgery. Dopaminergic medication was withdrawn the night before surgery. Subjects' demographic and clinical characteristics are provided in Table 1. All procedures were approved by the University of Pittsburgh Institutional Review Board (IRB Protocol # PRO13110420), and all patients provided informed consent to participate in the study.

[TABLE 1 ABOUT HERE]

Stimuli and procedure. Participants performed a reading-aloud task during the subcortical mapping portion of the surgery in up to 4 recording sessions per patient, with 120 trials per session. The visual stimuli consisted of consonant-vowel-consonant (CVC) words and pseudowords presented on a computer screen. The stimuli were chosen from an existing stimulus set, and were balanced along a number of psycholinguistic parameters, such as phonological and orthographic neighborhood density, bigram frequency, phonotactic and biphone probability, etc. (for a detailed description of the stimuli, see Moore, Fiez, and Tompkins, 2017). For the purposes of the present study, the stimuli were grouped into two categories based on the primary articulator involved in the production of the initial consonants:

words with word-initial labial consonants (i.e., those requiring closure or constriction of the air flow primarily with the use of the lips), and words with word-initial coronal consonants (i.e., those requiring articulation primarily with the use of the tongue). The labial consonants subsumed bilabial (/p/, /m/) and labiodental (/f/, /v/) phonemes; coronal consonants included alveolar (/s/, /z/, /t/, /d/, /l/, /n/), post-alveolar (/ʃ/, /r/), and dental (/θ/, /ð/) phonemes.

The stimuli were created and presented by custom code running in the Matlab environment (MathWorks, Natick, MA) using Psychophysics Toolbox extensions (Brainard, 1997). A schematic of the experimental procedure is shown in Figure 1. On each trial, participants were presented with a white cross against a black background during an intertrial interval, after which a green fixation cross appeared on the screen for 250 ms instructing the participants to get ready. It was followed by a variable interstimulus interval (500-1000 ms) during which the screen remained black. Then the stimulus word was presented on the screen and participants were instructed to read it out loud. The stimulus word remained on the screen until participants made the response, after which the experimenter advanced the presentation to the next trial. All stimuli (120 trials per recording session) were pseudorandomized in order of presentation. Participants were familiarized with the task prior to surgery.

[FIGURE 1 ABOUT HERE]

Audio recordings. Participants' reading aloud was recorded using an omnidirectional microphone (Audio-Technica ATR3350iS Mic, frequency response 50-18,000 Hz, or PreSonus PRM1 Mic, frequency response 20-20,000 Hz). The microphone was positioned at a distance of approximately 8 cm from the subject's left oral angle of the mouth and oriented at an angle of approximately 45 degrees. A Zoom H6 digital recorder was used to record the audio signal at a sampling rate of 96 kHz. This signal was simultaneously recorded using a Grapevine Neural

171 Interface Processor (Ripple LLC, Salt Lake City, UT, USA) at a lower sampling rate of 30 kHz.
172 The audio recordings were segmented and transcribed offline by phonetically-trained
173 communication science students using the International Phonetic Alphabet (IPA) in a custom-
174 designed graphical user interface (GUI) implemented in MATLAB. The audio recordings were
175 synchronized with the neural recordings using digital pulses delivered to the Neuro-Omega
176 system (Alpha Omega, Nazareth, Israel) via a USB data acquisition unit (Measurement
177 Computing, Norton, MA, model USB-1208FS).
178
179 ***Subthalamic nucleus recordings.*** Subjects were implanted with DBS leads bilaterally, but
180 local field potentials were recorded during the administration of the reading-aloud task only for
181 the left side surgery (see Figure 2A for an example of lead trajectory). The LFP signal was
182 acquired with the Neuro-Omega recording system using parylene insulated tungsten
183 microelectrodes (25 µm in diameter, 100 µm in length) with a stainless steel macroelectrode
184 ring (0.55 mm in diameter, 1.4 mm in length) 3 mm above the tip of the microelectrode. The LFP
185 signal was recorded at a sampling rate of 44 kHz and was band-pass filtered at 0.075 Hz to 10
186 kHz. The microelectrodes targeted the dorsolateral area of the STN, as previously described in
187 Lee et al. (2018). The microelectrodes were oriented on the microtargeting drive system using
188 two or three trajectories of a standard cross-shaped Ben-Gun array with a 2 mm center-to-
189 center spacing: for mapping of the center, posterior, and medial tracts. The microelectrodes
190 were advanced manually in 0.1 mm steps starting 10 mm above the defined target. The patients
191 were subsequently implanted with DBS Medtronic 3389 leads with four platinum-iridium
192 cylindrical macroelectrodes 1.27 mm in diameter, 1.5 mm in length and a 0.5 mm electrode
193 spacing (Medtronic, Minneapolis, MN, USA). The superior and inferior boundaries of the STN
194 were determined by the neurophysiologist and neurosurgeon based on the characteristic STN
195 single-unit neuronal activity obtained from the microelectrode recordings (MER). The speech
196 task was administered and LFP data acquired for up to four different depths within the STN per

patient. As a result, LFP data from a total of 79 recording sites were obtained across all patients, noting that for the most superficial recording sites within the STN, the macroelectrode ring may have been just superior to the dorsal border of STN. The locations of the macroelectrode contacts were determined using the semi-automatic approach implemented in the Lead-DBS toolbox (Horn and Kühn, 2015; Horn et al., 2019). In brief, post-operative CT scans were linearly coregistered with pre-operative MRI scans and normalized to MNI (Montreal Neurological Institute) space. MNI-defined coordinates of macroelectrode contact locations were extracted for all subjects and visualized in Figure 2B.

[FIGURE 2 ABOUT HERE]

***Cortical recordings*.** In addition to the clinical subcortical mapping procedure, all patients were also temporarily implanted with subdural electrode arrays over the cortical surface of the left hemisphere which were inserted through the burr hole after opening the dura, but before the insertion of subcortical guide tubes. The ECoG signal was acquired at 30 kHz using the Grapevine Neural Interface Processor. Most subjects were implanted with 6- or 28-channel Ad-Tech electrode strips (Ad-Tech Medical Corporation, Racine, WI, USA) except for two subjects who were implanted with either a 36- or 54-channel PMT electrode strips each (PMT Corporation, Chanhassen, MN, USA). Depending on the type of the electrodes, the electrodes varied 1, 2 or 4 mm in diameter, and 3, 4 or 10 mm in center-to-center spacing. The placement of the electrode strips was targeted at the ventral sensorimotor cortex by using stereotactic coordinates to mark the scalp over this region and advancing the subdural strips in the direction of this overlying visual marker. A total of 198 electrodes were placed on the cortex, but only 125 were included in the analyses – those that were confined to the sensorimotor cortex, as determined in the patients' native brain space (Figure 2C shows these locations in MNI space). Localization of the electrodes on the cortical surface was reconstructed from 1) the intra-

223 operative fluoroscopic images (512 × 512 pixels, General Electric, OEC 9900) and 2) the
224 coregistered pre-operative and post-operative computed tomography (CT) images obtained
225 after placement of the Leksell frame and 3) pre-operative magnetic resonance imaging (MRI)
226 scans according to the semi-automated method described in Randazzo et al. (2016). Electrode
227 locations were then registered to the common brain space using the MNI template (ICBM152)
228 with Brainstorm (Tadel et al., 2011) (https://neuroimage.usc.edu/brainstorm/). Subjects' MNI-
229 defined ECoG electrodes that were constrained to the sensorimotor cortex in native space are
230 presented in 3D MNI space in Figure 2D.
231
232 ***Data selection.*** Of the 11 subjects who participated in the study, STN data for one subject
233 (Subject 2) was not recorded due to a technical error. ECoG data from two subjects contained
234 excessive artifacts in the signal (Subjects 7 and 10) and were excluded from the analysis. Trials
235 were included in the analysis if 1) a student coding the data was able to unambiguously identify
236 a subject's spoken response; 2) a subject's spoken response constituted the stimuli's targeted
237 CVC structure; 3) a subject's response included the stimuli's targeted phonemes. On the basis
238 of these criteria, 359 (9.8%) out of a total of 3,669 recorded trials were rejected.
239
240 ***Electrophysiological data processing***. Data processing was performed using custom code
241 based on the Statistical Parametric Mapping (SPM12) (Wellcome Department of Cognitive
242 Neurology, London, UK) (http://www.fil.ion.ucl.ac.uk/spm/software/spm12/) and Fieldtrip
243 (Oostenveld et al., 2011) toolboxes implemented in MATLAB. The data were resampled to a
244 sampling frequency of 1 kHz. In order to minimize noise and artifactual electrode cross-talk in
245 the signal, the data were re-referenced offline using a common average referencing procedure
246 applied over blocks of electrodes connected by the same headstage connector for the ECoG
247 recordings, and using a common average referencing procedure for the STN recordings. A 1 Hz
248 high-pass filter and a 58-62 Hz notch filter were applied to remove cardioballistic artifacts and

line noise, respectively. The signal was then aligned with the presentation of the green cross cue for subsequent baseline epoching and with the vowel onset (the transition between the initial consonant and the subsequent vowel, CV) for speech response epoching. The CV transition was used to separate the consonantal component from the subsequent vocalic component in subjects' spoken responses (as in Bouchard et al., 2013). For artifact rejection, data were visually inspected over 6000-ms long time windows surrounding baseline and vowel onset; time widows with residual artifacts and excessive noise were excluded from analysis, resulting in an additional 4.8% data rejection. The remaining data underwent a time-frequency transformation using Morlet wavelets with 7 cycles over frequencies between 1 and 200 Hz in incrementing steps of 2 Hz. The resulting signal was normalized using z-scores calculated relative to a 1000-ms long baseline period (250 ms before and 750 ms after green cross presentation). A time-varying analytic amplitude in the high gamma frequency range (60-150 Hz) was extracted for further analyses because it has been consistently reported to reflect changes in sensory, motor and cognitive functions, including speech (e.g., Bouchard et al., 2013; Crone et al., 1998; Edwards et al., 2005).

Experimental design and statistical analysis. All statistical analyses were performed in MATLAB 2017a and R version 3.4.4 (R Development Core Team, 2018). A within-subjects experimental design was used, in which all subjects (n = 11) received trials with both lips and tongue articulations (120 trials per recording session). Recorded LFPs from the sensorimotor cortex and the subthalamic nucleus were analyzed separately using the same statistical procedures. For the analysis of the LFPs throughout speech production, a time window of 1000 ms (500 ms before and 500 ms after the vowel onset) encompassing subjects' whole spoken response was used. For the analysis of the articulatory specificity of the initial consonant, a 500-ms time window preceding the vowel onset was used. Although durations of the word-initial consonants (as measured from the acoustic output) were on average 130 ms (coronal

consonants: 139 ms, labial consonants: 106 ms, $t(46799) = -42.29$, $p < 0.001$), a broader time window of 500 ms allowed examination of potential pre-articulatory neuronal activity. To analyze high gamma activity elicited during the speech task, a series of fitted linear mixed effects models (LMEMs) with restricted maximum likelihood estimation were carried out using lme4 (Bates, Maechler, Bolker, and Walker, 2015) and lmerTest (Kuznetsova, Brockhoff, and Christensen, 2017) packages. Subjects were entered as random effects to account for subject-specific idiosyncrasies. Model comparisons were performed via backward elimination of fixed effects and their interactions in order to measure the goodness of model fit without unnecessary parameter overfitting using the Akaike information criterion (Akaike, 1974). To perform correlation analyses between the observed speech and articulatory response and electrode location coordinates in the MNI space, we applied a Spearman's rank correlation test. Generally, to assess statistical differences of speech-related changes in the brain response, we used Welch two sample t-tests when the data were found not to deviate significantly from normality; when the data were not normally distributed, nonparametric Wilcoxon rank sum or Wilcoxon signed-rank (to determine the significance of response compared to baseline) tests were used. To assess normality of the data distribution, a one-sample Kolmogorov-Smirnov test was used; a two-sample Kolmogorov-Smirnov test was used to compare STN and cortical datasets. False discovery rate (FDR) method (as described in Benjamini and Hochberg, 1995) was used at $\alpha = 0.05$ to control for multiple comparisons. Effect sizes were estimated with Hedges' g (Hedges, 1981); effects larger than 0.5 were considered large, according to Sawilowsky (2009).

RESULTS

Behavioral response. Subjects' behavioral performance is summarized in Table 2. Across subjects, the mean latency from seeing the stimulus word on the screen to producing the word was 1.34 ± 0.51 s; the mean duration of the spoken response was 0.59 ± 0.16 s. The severity of

the disease symptoms as measured by the UPDRS off medication did not account for variation in response latency (estimated coefficient = -0.006, SE = 0.018, t = -0.23, p = 0.77) or response duration (estimated coefficient = -0.003, SE = 0.005, t = -0.63, p = 0.54). Average response accuracy was 88.5%, although subjects 1, 2, and 7 produced many non-target responses (incomplete words and/or non-target phonemes) resulting in a high percent of rejected trials (more than 20%).

[TABLE 2 ABOUT HERE]

Speech-related activity. STN LFP activity showed significant time-frequency modulations relative to baseline (Figure 3A) that were comparable with those obtained from the sensorimotor cortex (Figure 3B). There were significant decreases in z-scored spectral power in the alpha (8-12 Hz) and beta (12-30 Hz) frequency bands and significant increases in z-scored power at high frequency ranges relative to baseline, as determined by the Wilcoxon signed-rank test (α = 0.05, FDR corrected). Increases in the spectral power occurred from 60 Hz to180 Hz for STN sites, and from 50Hz and onward for the cortical sites. In both cases, significant high frequency modulations occurred around 400 ms before speech onset and persisted until about 100 ms before speech offset for STN activity and until about 100 ms after speech offset for sensorimotor cortex activity. A more detailed examination of the z-scored spectral power in the high gamma frequency range over the spoken response window (500 ms before vowel onset and 500 ms after vowel onset) showed that in 86% (68/79) of STN sites and 95% (119/125) of sensorimotor cortex ECoG sites, high gamma power was significantly greater than baseline (Wilcoxon signed-rank test at α = 0.05, FDR corrected). Significant increases in average high gamma power during speech production were observed in all patients in both structures. The subjects' symptom severity (as measured by a total UPDRS score) was not correlated (Spearman's rank-order correlation test) with the average high gamma activity for the speech response window

either in the STN ($r_s(10) = 0.37$, $p = 0.29$) or the sensorimotor cortex ($r_s(9) = 0.43$, $p = 0.24$). In the STN, averaged high gamma power significantly correlated with the location of recording sites along the ventral-dorsal axis in the MNI space ($r_s(79) = 0.53$, $p < 0.001$) and anterior-posterior axis ($r_s(79) = 0.36$, $p = 0.0012$), but not the lateral-medial axis ($r_s(79) = 0.03$, $p = 0.78$). In contrast, we found no significant correlation between high gamma power and the location of the recording sites on the sensorimotor cortex. To explain the observed variation in the high gamma power across STN recording sites and to control for subject variability, we fitted linear mixed effects models (LMEM). The most parsimonious model included average high gamma power as a dependent variable, subjects as a random effect, and the location of recording sites along the ventral-dorsal axis (the MNI-defined Z coordinate) as a fixed effect. The outcome of the LMEM suggests that, even after taking subject-to-subject variability into account, high gamma power changed significantly from dorsal to ventral parts of the STN, with greater high gamma power observed dorsally (estimated coefficient = 0.017, SE = 0.005, $t = 3.19$, $p = 0.004$). Mixed effects modeling of the high gamma response in the sensorimotor cortex did not yield significant effects.

[FIGURE 3 ABOUT HERE]

Representation of articulators. To examine the spatial distribution of speech articulator representations within the STN and sensorimotor cortex, we compared (Welch two sample t-test) high gamma power averaged over the prevocalic time window of 500 ms for trials with word-initial coronal (tongue) consonants vs. trials with word-initial labial (lips) consonants, at each recording site. We used the outcome of the t-test and the sign of the t-value to detect discriminative articulatory activity. For example, a significant ($\alpha = 0.05$) and positive t-value indicated that a given site's average high gamma power was greater for consonants articulated with the lips than those articulated with the tongue; conversely, negative t-values indicated

353 tongue-related activity. MNI-defined locations of cortical and STN articulator-responsive sites
354 are plotted in Figures 4A and C, respectively. An example of what constituted articulator-
355 discriminative activity is shown for representative recording sites in Figures 4B and D. The
356 remaining sites at which a significant increase in high gamma power was observed produced an
357 undifferentiated activity, i.e. they were equally active during articulation of both coronal and
358 labial consonants. The discriminative sites within the STN included 18 (23%) out of a total of 79
359 electrodes: 5 sites exhibited greater high gamma activity during articulation with the lips; 13
360 sites were most active during articulation with the tongue; the discriminative cortical sites
361 included 37 (30%) out of a total of 125 electrodes: 19 sites showed lips-preferred activity and 18
362 sites showed tongue–preferred activity (Figure 5C). Of the eight subjects with both STN and
363 cortical data, three were found to have articulator-discriminative sites in both STN and
364 sensorimotor cortex; two subjects showed articulator-discriminative activity only in the STN; two
365 subjects had discriminative sites only in the sensorimotor cortex, and 1 subject did not show
366 discriminative sites in either of the structures. One subject who only had ECoG data showed
367 articulator-discriminative sites. Of the two remaining subjects who only had STN data,
368 articulator-discriminative sites were observed only for one patient. In the STN, recording sites
369 with tongue-preferred activity appeared to be located more dorsally compared to those selective
370 for lips; however, the obtained t-values did not correlate significantly with any of the three spatial
371 orientation planes through the recording locations (ventrodorsal, anteroposterior, or
372 lateromedial), according to a Spearman's rank-order correlation test. Modeling of the articulatory
373 activity in the STN with mixed effects regression approach did not yield significant effects (the
374 most parsimonious model included subjects as a random effect and recording locations along
375 the lateral-medial axis, the MNI-defined X coordinate, as a fixed effect). In the sensorimotor
376 cortex, t-values correlated significantly with the location of recording sites along the ventral-
377 dorsal ($r_s(125) = -0.39$, $p < -0.001$) and lateral-medial ($r_s(125) = -0.35$, $p = < 0.001$) axes.
378 Modeling the articulatory effect with LMEMs produced similar results. Keeping subjects as a

379 random effect, the most parsimonious models yielded a significant effect of the recording
380 location along the ventral-dorsal (estimated coefficient = 0.064, SE = 0.022, t = 2.98, p = 0.004)
381 and the lateral-medial (estimated coefficient = 0.148, SE = 0.053, t = 2.6, p = 0.011) axes. Thus,
382 taking subject-to-subject differences into account, the articulator-related activity in the
383 sensorimotor cortex appeared to be somatotopically organized, with the recording sites
384 exhibiting encoding of lip articulations located more dorsally (and medially due to the cortex
385 curvature), and sites exhibiting encoding of tongue articulations distributed more broadly over
386 the ventrolateral part of the sensorimotor cortex.
387
388 [FIGURE 4 ABOUT HERE]
389
390 To quantify the time-course of the articulatory neural encoding, we examined the distribution of
391 average high gamma activity for all tongue vs. lips trials at the identified articulator-
392 discriminative sites in the STN (n = 18) and the sensorimotor cortex (n = 37) (Figures 5A and B).
393 A two-sample Kolmogorov-Smirnov test showed that the STN and cortical data had significantly
394 different distributions: $D(55) = 0.22$, $p < 0.001$. In the sensorimotor cortex, high gamma activity
395 for both tongue and lips trials was more tightly distributed and peaked around the time of vowel
396 onset, whereas activity in the STN had two peaks: approximately 80 ms before consonant onset
397 and 120 ms after vowel onset. The second, postvocalic peak in high gamma activity in the STN
398 may reflect activity related to the articulation of the word-final consonant. However, because our
399 stimulus set was not designed to counterbalance lip and tongue features across all the
400 phonemes in each syllable, we cannot rule out other possibilities, such as activity related to
401 vowel articulation or midword co-articulatory processes. In the prevocalic 500-ms window
402 corresponding to the consonants of interest, the time of peak high gamma activity in the STN
403 preceded that in the sensorimotor cortex (sensorimotor cortex: mean peak time = -0.07 s, SD =
404 0.08 s; STN: mean peak time = -0.16 s, SD = 0.1 s), $t(27.64) = 3.36$, $p = 0.002$). The mean

405 change in amplitude of high gamma activity in the 500-ms time window was significantly greater
406 at cortical sites (mean = 0.98, SD = 0.79) compared to STN sites (mean = 0.58, SD = 0.41):
407 $t(52.65) = 2.51$, $p = 0.02$). Within the STN, mean high gamma amplitude was greater during the
408 tongue trials (mean = 0.3, SD = 0.19) compared to the lips trials (mean = 0.17, SD = 0.06):
409 ($t(20.83) = 2.74$, $p = 0.012$), whereas no difference in high gamma amplitude between the two
410 articulators was observed at cortical sites.
411
412 Additionally, in order to identify the times at which the difference in high gamma activity for
413 tongue vs. lips articulations was the largest, regardless of the underlying magnitude of high
414 gamma activity, we estimated its effect size (Hedges' *g*) for each articulator-discriminative site at
415 each time point (n = 51, $\Delta t = 40$ ms) within the 2 s interval centered at vowel onset. Effect sizes
416 indicating presence of articulatory discrimination at a given time point are plotted in Figure 5D.
417 In contrast to the timing of the overall high gamma activity in sensorimotor cortex, which peaked
418 near vowel onset, the greatest articulatory discrimination was observed near consonant onset
419 (mean time = -0.12 s, SD = 0.09). Maximum discrimination was observed even earlier in the
420 STN, approximately 120 ms before consonant onset (mean time = -0.24 s, SD = 0.14): $t(25.1) =$
421 3.19, $p = 0.004$ (Figure 5D), where the mean magnitude of the effect also was significantly
422 greater (mean = 1.94, SD = 1.01) than in sensorimotor sites (mean = 1.06, SD = 0.84): $t(29.02)$
423 $= -3.2$, $p = 0.003$).
424
425 [FIGURE 5 ABOUT HERE]
426
427 **Discussion**
428 We analyzed LFPs obtained from the simultaneous recording of the cortical and STN activity in
429 11 human subjects with Parkinson's disease while they participated in a speech task during
430 subcortical mapping for the implantation of DBS electrodes. We selected the speech stimuli

such that articulation of the initial consonant engaged either tongue or lip musculature, in order to examine whether encoding of speech articulators, similar to that previously reported for the sensorimotor cortex, is represented in subthalamic high gamma activity. We found that STN high gamma activity tracks speech production at the level of vocal tract articulators, which occurs prior to the onset of vocalization and often prior to related cortical encoding.

Speech-related activation. We found that speech production was accompanied by significant time-frequency modulations in both the STN and the sensorimotor cortex, namely, suppression of alpha and beta activity and increase in high gamma activity (above 50 Hz). In both cases, significant time-frequency modulations emerged about 400 ms before spoken response onset and persisted throughout the execution of speech. Decrease of activity in the alpha and beta bands and increase of activity in high frequency bands have been previously reported as markers of ongoing movement and movement-related patterns in the STN (Androulidakis et al., 2007; Kempf et al., 2007; Lipski et al., 2017; Geng et al., 2018; Lofredi et al., 2018). However, only modulation of beta activity during speech production has been reported (Hebb, Darvas, and Miller, 2012). Thus, our results provide the first demonstration of evoked increases in STN high gamma activity before and during speech production. Importantly, we show that the power of high gamma response changes significantly along the dorsoventral plane of the MNI-defined locations of the STN electrodes, with greater high gamma power observed dorsally. This finding agrees with recent demonstration that subthalamic gamma power is greatest in the sensorimotor part of the STN (Lofredi et al., 2018). Thus, in light of the existing conception of the parcellated organization of the STN into sensorimotor, associative, and limbic areas (Hamani et al., 2004; Temel et al., 2005; Haynes and Haber, 2013), our results show that articulatory aspects of speech recruit the sensorimotor region of the STN, and are in line with our previous findings showing speech-related increases in the firing rate of human STN neurons (Lipski et al., 2018). In contrast to the STN, the magnitude of cortical high gamma activity was

not significantly different across recording locations. Given that the cortical recordings were confined to the orofacial segment of the sensorimotor cortex and the evidence of overlapping speech-related activation in the precentral and postcentral gyri (Penfield and Boldrey, 1937; Bouchard et al., 2013; Breshears et al., 2015), this lack of spatial differentiation in the cortical high gamma activity is not unexpected.

Encoding of speech articulators. In order to further quantify the observed speech-related high gamma modulation in the STN and the sensorimotor cortex, we examined whether the two structures showed encoding specific to speech articulators. For the sensorimotor cortex, we found that 30% of recording sites revealed either lips-preferred or tongue-preferred activity, which had a topographic distribution: the electrodes located more dorsally on the sensorimotor cortex produced a greater high gamma power during the articulation of lips consonants while the electrodes that were located more ventrally yielded a greater high gamma power for tongue consonants. Thus, our results appear to recapitulate the dorsoventral layout for lips and tongue representations within the sensorimotor cortex (Penfield and Boldrey, 1937; Bouchard et al., 2013; Breshears et al., 2015; Chartier et al., 2018; Conant et al., 2018). We found that articulatory encoding is closely aligned with the consonant onset in acoustic speech production. This discriminative activity began to emerge about 500 ms before articulation, suggesting the potential encoding of pre-articulatory preparatory processes like planning a motor command and retrieving the sensory representation of the intended articulatory target (Guenther, Ghosh, and Tourville, 2006). For the STN, we found that 23% of recording locations showed articulator-discriminative activity, but without articulatory somatotopy. Previous studies demonstrating functional organization in the STN of human and nonhuman primates have used single unit recordings to demonstrate a crude somatotopy for arm-related and leg-related movements (Monakow et al., 1978; DeLong et al., 1985; Wichmann et al., 1994; Nambu, Takada, Inase, and Tokuno, 1996; Rodriguez-Oroz et al., 2001; Starr et al., 2003; Theodosopoulos et al., 2003),

483 although representations for face, eyes and finer-grained movements with shoulders, elbows,
484 knees, wrists, etc. have been less somatotopically consistent (e.g., DeLong et al., 1985;
485 Wichmann et al., 1994). It should be noted that LFP recordings might not be expected to
486 delineate a functional somatotopy, due to their representation of group level neuronal activity
487 recorded from a much larger volume of tissue than the signal obtained from microelectrode
488 recordings. In this respect, it is remarkable that we found evidence for articulator-level encoding
489 in the LFP signal, which may indicate the encoding of aspects of speech production that are
490 specific to these articulatory maneuvers but separate from their anatomical representation at the
491 cortical level.
492
493 The time-course of the articulatory encoding in the STN further supports a differentiation from
494 sensorimotor cortex. We found that high gamma activity at articulator-discriminative STN
495 recording sites had two peaks approximately 320 ms apart: an early one (~80 ms) before
496 acoustically defined speech onset and a later one (~240 ms) after speech onset. Because all
497 stimulus words were of the CVC type, such pattern of activity may reflect a transient rather than
498 a sustained type of activation at consonant onsets (see Salari et al., 2018). Alternatively, the
499 second peak of activity could be vowel-related since some of the stimulus vowels included
500 articulation with lips in addition to tongue movements (e.g., lip rounding in /u/). It is also possible
501 that the observed pattern of activity in the STN reflects activity from multiple populations of
502 neurons with different speech-related functions that manifests itself with different peak latencies.
503 However, because the stimuli were not designed to tease apart these influences, a definitive
504 conclusion cannot be drawn from the data. Of note, we also found that articulatory
505 discrimination reflected in STN high gamma activity was not maximal near consonant onset, as
506 occurred in the sensorimotor cortex, but peaked about 120 ms before its acoustic production,
507 pointing at the possible involvement of the STN in articulator-specific planning (Figure 5D).
508 Although the finding of the relative temporal differences in the articulatory encoding between the

sensorimotor cortex and the STN is important, it is worth noting that we relied upon the phonetic coding of the produced acoustics to infer which articulators were involved in consonant productions (as in Bouchard et al., 2013). For a more precise characterization of the temporal aspects of the articulatory encoding, direct measurements of articulatory kinematics would be necessary, which were beyond the scope of the present study and are difficult to implement during DBS surgery. Thus, it remains to be established whether the observed articulator-related STN activity is indicative of the activation of musculature engaged in articulation and of a more mechanistic involvement of STN in speech articulation, or of its role in higher-order articulation-related processes, such as speech planning, control of kinematic trajectories, and switching between motor commands.

Limitations

We acknowledge that the disease state is a potential confound to our results. We do not report control data collected from a non-PD population. Given that basal ganglia activity in PD patients is characterized by reorganization of receptive fields and loss of specificity (Abosch et al., 2002; Hamani et al., 2004), we may be assessing an unknown amount of crosstalk or “motor overflow” of the signal related to different body parts (Bergman et al., 1998; Nambu, 2011). Additionally, we searched for articulator-specific somatotopy on the basis of 79 available STN recording locations with non-systematic spatial separation, which may represent inadequate sampling. Note that fine-wire EMG is not an option in awake neurosurgical patients, thus our experimental design did not allow us to measure articulatory muscle movement for correlation with intracranial signals. The potential encoding of other linguistic features, such as manner of articulation, also is an interesting question, but our stimulus set does not systematically sample them to adequately address this question. In ongoing work, we have developed new materials that more systematically engage consonant feature space, including manner, as well as vowel features, in the context of two behaviors: listening to speech vs. articulation of speech.

535

536 **Summary**

537 These data are the first to demonstrate time-frequency modulations in STN activity that track
538 articulatory aspects of speech, complimenting recent evidence for speech-related changes in
539 the timing and the firing rate of the STN neurons (Lipski et al., 2018). A major strength of this
540 study is the application of a single analytic approach to simultaneous LFP recordings from the
541 sensorimotor cortex and the STN, which allowed us to compare the neural activity in these brain
542 regions during speech. After demonstrating the expected somatotopic differentiation of vocal
543 tract articulators in the sensorimotor cortex, we showed that the STN also differentially encodes
544 speech articulators with more detailed temporal patterning that does not mirror cortical activity.
545 Further elucidation of the role of cortico-basal ganglia interactions in the speech production
546 network will be critical for improving our understanding of the neurobiology of speech
547 dysfunction in basal ganglia disorders and related future treatments.

548 **REFERENCES**

549 Abosch A, Hutchison WD, Saint-Cyr JA, Dostrovsky JO, Lozano AM (2002) Movement-related
550 neurons of the subthalamic nucleus in patients with Parkinson disease. J Neurosurg
551 97:1167–1172.
552 Akaike H (1974) A new look at the statistical model identification. IEEE Transactions on
553 Automatic Control 19:716–723.
554 Aldridge D, Theodoros D, Angwin A, Vogel AP (2016) Speech outcomes in Parkinson's disease
555 after subthalamic nucleus deep brain stimulation: A systematic review. Parkinsonism
556 Relat Disord 33:3–11.
557 Alexander GE, DeLong MR, Strick PL. (1986) Parallel organization of functionally segregated
558 circuits linking basal ganglia and cortex. Annu Rev Neurosci 9:357–81.
559 Androulidakis AG, Kühn AA, Chen CC, Blomstedt P, Kempf F, Kupsch A, ... Brown P (2007)
560 Dopaminergic therapy promotes lateralized motor activity in the subthalamic area in
561 Parkinson's disease. Brain, 130:457-468.
562 Bates D, Maechler M, Bolker B, Walker S (2015) Fitting linear mixed-effects models using lme4.
563 Journal of Statistical Software 67:1-48.
564 Benjamini Y, Hochberg Y (1995) Controlling the false discovery rate: A practical and powerful
565 approach to multiple testing. Journal of the Royal Statistical Society 57:289-300.
566 Bergman H, Feingold A, Nini A, Raz A, Slovin H, Abeles M, Vaadia E (1998) Physiological
567 aspects of information processing in the basal ganglia of normal and parkinsonian
568 primates. Trends in neurosciences 21:32-38.
569 Bouchard KE, Chang EF (2014) Control of spoken vowel acoustics and the influence of
570 phonetic context in human speech sensorimotor cortex. Journal of Neuroscience
571 34:12662-12677.

572 Bouchard KE, Conant DF, Anumanchipalli GK, Dichter B, Chaisanguanthum KS, Johnson K,
573 Chang EF (2016) High-resolution, non-invasive imaging of upper vocal tract articulators
574 compatible with human brain recordings. PLoS One 11:e0151327.
575 Bouchard KE, Mesgarani N, Johnson K, Chang EF (2013) Functional organization of human
576 sensorimotor cortex for speech articulation. Nature 495:327-332.
577 Brainard DH (1997) The Psychophysics Toolbox. Spatial Vision 10:433-436.
578 Breshears JD, Molinaro AM, Chang EF (2015) A probabilistic map of the human ventral
579 sensorimotor cortex using electrical stimulation. Journal of Neurosurgery 123:340-349.
580 Brown S, Ngan E, Liotti M (2007) A larynx area in the human motor cortex. Cerebral Cortex
581 18:837-845.
582 Brunner RJ, Kornhuber HH, Seemtiller E, Suger G, Wallesch CW (1982) Basal ganglia
583 participation in language pathology. Brain and Language 16:281-299.
584 Carey D, Krishnan S, Callaghan MF, Sereno MI, Dick F (2017) Functional and quantitative MRI
585 mapping of somatomotor representations of human supralaryngeal vocal tract. Cerebral
586 Cortex 27:265-278.
587 Chartier J, Anumanchipalli GK, Johnson K, Chang EF (2018) Encoding of articulatory kinematic
588 trajectories in human speech sensorimotor cortex. Neuron 98:1042-1054.
589 Cheung C, Hamilton LS, Johnson K, Chang EF (2016) The auditory representation of speech
590 sounds in human motor cortex. Elife 5:e12577.
591 Conant DF, Bouchard KE, Leonard MK, Chang EF (2018) Human sensorimotor cortex control of
592 directly-measured vocal tract movements during vowel production. Journal of
593 Neuroscience 2382-17.
594 Crone NE, Miglioretti DL, Gordon B, Lesser RP (1998) Functional mapping of human
595 sensorimotor cortex with electrocorticographic spectral analysis: II. Event-related
596 synchronization in the gamma band. Brain 121:2301-2315.

597 Damasio AR, Damasio H, Rizzo M, Varney N, Gersh F (1982) Aphasia with nonhemorrhagic
598 lesions in the basal ganglia and internal capsule. Arch Neurol 39:15–24.
599 DeLong MR, Crutcher MD, Georgopoulos AP (1985) Primate globus pallidus and subthalamic
600 nucleus: functional organization. Journal of Neurophysiology 53:530-543.
601 Edwards E, Soltani M, Deouell LY, Berger MS, Knight RT (2005) High gamma activity in
602 response to deviant auditory stimuli recorded directly from human cortex. Journal of
603 Neurophysiology 94:4269-4280.
604 Ewert S, Plettig P, Li N, Chakravarty MM, Collins DL, Herrington TM, ... Horn A (2017) Toward
605 defining deep brain stimulation targets in MNI space: A subcortical atlas based on
606 multimodal MRI, histology and structural connectivity. NeuroImage 170: 271-282.
607 Geng X, Xu X, Horn A, Li N, Ling Z, Brown P, Wang S (2018) Intra-operative characterisation of
608 subthalamic oscillations in Parkinson's disease. Clinical Neurophysiology 129:1001-
609 1010.
610 Guenther FH, Ghosh SS, Tourville JA (2006) Neural modeling and imaging of the cortical
611 interactions underlying syllable production. Brain and Language 96:280-301.
612 Hamani C, Saint-Cyr JA, Fraser J, Kaplitt M, Lozano AM (2004) The subthalamic nucleus in the
613 context of movement disorders. Brain 127:4-20.
614 Haynes WI, Haber SN (2013) The organization of prefrontal-subthalamic inputs in primates
615 provides an anatomical substrate for both functional specificity and integration:
616 implications for Basal Ganglia models and deep brain stimulation. Journal of
617 Neuroscience 33:4804-4814.
618 Hebb AO, Darvas F, Miller KJ (2012) Transient and state modulation of beta power in human
619 subthalamic nucleus during speech production and finger movement. Neuroscience
620 202:218-233.
621 Hedges LV (1981) Distribution theory for Glass' estimator of effect size and related estimators.
622 Journal of Educational Statistics 6:107–128.

623 Hesselmann V, Sorger B, Lasek K, Guntinas-Lichius O, Krug B, Sturm V, ... Lackner K (2004)
624 Discriminating the cortical representation sites of tongue and lip movement by functional
625 MRI. Brain Topography 16:159-167.
626 Ho AK, Iansek R, Marigliani C, Bradshaw JL, Gates S (1998) Speech impairment in a large
627 sample of patients with Parkinson's disease. Behav Neurol 11:131–137.
628 Horn A, Kühn AA (2015) Lead-DBS: a toolbox for deep brain stimulation electrode localizations
629 and visualizations. Neuroimage 107:127–135.
630 Horn A, Li N, Dembek TA, Kappel A, Boulay C, Ewert S, ... Reisert M (2019) Lead-DBS v2:
631 Toward a comprehensive pipeline for deep brain stimulation imaging. NeuroImage
632 184:293–316.
633 Kempf F, Kühn AA, Kupsch A, Brücke C, Weise L, Schneider GH, Brown P (2007)
634 Premovement activities in the subthalamic area of patients with Parkinson's disease and
635 their dependence on task. European Journal of Neuroscience 25:3137-3145.
636 Knowles T, Adams S, Abeyesekera A, Mancinelli C, Gilmore G, Jog M (2018) Deep brain
637 stimulation of the subthalamic nucleus parameter optimization for vowel acoustics and
638 speech intelligibility in Parkinson's disease. Journal of Speech, Language, and Hearing
639 Research 61:510-524.
640 Kuznetsova A, Brockhoff PB, Christensen RHB (2017). lmerTest package: Tests in linear mixed
641 effects models. Journal of Statistical Software 82:1-26.
642 Lee PS, Weiner GM, Corson D, Kappel J, Chang YF, Suski VR, ... & Richardson RM (2018)
643 Outcomes of interventional-MRI versus microelectrode recording-guided subthalamic
644 Deep Brain Stimulation. Frontiers in Neurology 9:241.
645 Lipski WJ, Alhourani A, Pirnia T, Jones PW, Dastolfo-Hromack C, Helou LB, ... Richardson RM
646 (2018) Subthalamic nucleus neurons differentially encode early and late aspects of
647 speech production. Journal of Neuroscience, 38:5620-5631.

Lipski WJ, Wozny TA, Alhourani A, Kondylis ED, Turner RS, Crammond DJ, Richardson RM (2017) Dynamics of human subthalamic neuron phase-locking to motor and sensory cortical oscillations during movement. Journal of Neurophysiology 118:1472-1487.

Lofredi R, Neumann WJ, Bock A, Horn A, Huebl J, Siegert S, ... Kühn AA (2018) Dopamine-dependent scaling of subthalamic gamma bursts with movement velocity in patients with Parkinson's disease. Elife 7:e31895.

Logemann JA, Fisher HB, Boshes B, Blonsky ER (1978) Frequency and co-occurrence of vocal tract dysfunctions in the speech of a large sample of Parkinson patients. J Speech Hear Disord 43:47–57.

Lotte F, Brumberg JS, Brunner P, Gunduz A, Ritaccio AL, Guan C, Schalk G (2015) Electrocorticographic representations of segmental features in continuous speech. Frontiers in Human Neuroscience 9:97.

Lotze M, Seggewies G, Erb M, Grodd W, Birbaumer N (2000) The representation of articulation in the primary sensorimotor cortex. Neuroreport 11: 2985-2989

Meier JD, Aflalo TN, Kastner S, Graziano MS (2008) Complex organization of human primary motor cortex: a high-resolution fMRI study. Journal of Neurophysiology 100:1800-1812.

Monakow HWK, Akert K, Kiinzle H (1978) Projections of the precentral motor cortex and other cortical areas of the frontal lobe to the subthalamic nucleus in the monkey. Exp. Brain Res 33:395-403.

Moore MW, Fiez JA, Tompkins CA (2017) Consonant age-of-acquisition effects in nonword repetition are not articulatory in nature. J Speech Lang Hear Res 60:3198 –3212.

Morrison CE, Borod JC, Perrine K, Beric A, Brin MF, Rezai A, Kelly P, Sterio D, Germano I, Weisz D, Olanow CW (2004) Neuropsychological functioning following bilateral subthalamic nucleus stimulation in Parkinson's disease. Arch Clin Neuropsychol 19:165–181.

673 Mugler EM, Patton JL, Flint RD, Wright ZA, Schuele SU, Rosenow J, ... Slutzky MW (2014)
674 Direct classification of all American English phonemes using signals from functional
675 speech motor cortex. Journal of Neural Engineering 11:035015.
676 Nadeau SE, Crosson B (1997) Subcortical aphasia. Brain Lang 58:355– 402
677 Nambu A (2011) Somatotopic organization of the primate basal ganglia. Frontiers in
678 Neuroanatomy 5:26.
679 Nambu A, Takada M, Inase M, Tokuno H (1996) Dual somatotopical representations in the
680 primate subthalamic nucleus: evidence for ordered but reversed body-map
681 transformations from the primary motor cortex and the supplementary motor area.
682 Journal of Neuroscience 16:2671-2683.
683 Oostenveld R, Fries P, Maris E, Schoffelen J-M (2011) FieldTrip: Open source software for
684 advanced analysis of MEG, EEG, and invasive electrophysiological data. Comput Intell
685 Neurosci 2011:156869.
686 Penfield W (1954) Mechanisms of voluntary movement. Brain 77:1-17
687 Penfield W, Boldrey E (1937) Somatic motor and sensory representation in the cerebral cortex
688 of man as studied by electrical stimulation. Brain 60:389-443.
689 Pulvermüller F, Huss M, Kherif F, del Prado Martin FM, Hauk O, Shtyrov Y (2006) Motor cortex
690 maps articulatory features of speech sounds. Proceedings of the National Academy of
691 Sciences 103:7865-7870.
692 R Core Team (2018) R: A language and environment for statistical computing. R foundation for
693 statistical computing, Vienna, Austria. URL https://www.R-project.org/
694 Ramsey NF, Salari E, Aarnoutse EJ, Vansteensel MJ, Bleichner MB, Freudenburg ZV (2017)
695 Decoding spoken phonemes from sensorimotor cortex with high-density ECoG grids.
696 NeuroImage 180: 301-311

697 Randazzo MJ, Kondylis ED, Alhourani A, Wozny TA, Lipski WJ, Crammond DJ, Richardson RM
698 (2016) Three-dimensional localization of cortical electrodes in deep brain stimulation
699 surgery from intraoperative fluoroscopy. Neuroimage 125:515-521.
700 Rodriguez-Oroz MC, Rodriguez M, Guridi J, Mewes K, Chockkman V, Vitek J, DeLong MR,
701 Obeso JA (2001) The subthalamic nucleus in Parkinson's disease: Somatotopic
702 organization and physiological characteristics. Brain 124:1777–1790.
703 Salari E, Freudenburg ZV, Vansteensel MJ, Ramsey NF (2018) Spatial-temporal dynamics of
704 the sensorimotor cortex: Sustained and transient activity. IEEE Transactions on Neural
705 Systems and Rehabilitation Engineering 26:1084-1092.
706 Sawilowsky S (2009) New effect size rules of thumb. Journal of Modern Applied Statistical
707 Methods 8: 467–474.
708 Starr PA, Theodosopoulos PV, Turner R (2003) Surgery of the subthalamic nucleus: use of
709 movement-related neuronal activity for surgical navigation. Neurosurgery 53:1146-1149.
710 Tadel F, Baillet S, Mosher JC, Pantazis D, Leahy RM (2011) Brainstorm: A User-Friendly
711 Application for MEG/EEG Analysis. Computational Intelligence and Neuroscience 8.
712 Takai O, Brown S, Liotti M (2010) Representation of the speech effectors in the human motor
713 cortex: somatotopy or overlap? Brain and language 113:39-44.
714 Temel Y, Blokland A, Steinbusch HW, Visser-Vandewalle V (2005) The functional role of the
715 subthalamic nucleus in cognitive and limbic circuits. Prog Neurobiol 76:393–413.
716 Theodosopoulos PV, Marks WJ, Christine C, Starr PA (2003) The locations of movement-
717 related cells in the human subthalamic nucleus in Parkinson's disease. Movement
718 Disorders 18:791–798.
719 Wallesch CW, Kornhuber HH, Brunner RJ, Kunz T, Hollerbach B, Suger G (1983) Lesions of the
720 basal ganglia, thalamus, and deep white matter: Differential effects on language
721 functions. Brain and Language 20:286-304.

722 Walsh B, Smith A (2012) Basic parameters of articulatory movements and acoustics in
723 individuals with Parkinson's disease. Movement Disorders 27:843-850.
724 Watson P, Montgomery Jr EB (2006) The relationship of neuronal activity within the sensori-
725 motor region of the subthalamic nucleus to speech. Brain and Language 97:233-240.
726 Wichmann T, Bergman H, DeLong MR (1994) The primate subthalamic nucleus. I. Functional
727 properties in intact animals. Journal of Neurophysiology 72:494-506.
728 Witt K, Daniels C, Reiff J, Krack P, Volkmann J, Pinsker MO, Krause M, Tronnier V, Kloss M,
729 Schnitzler A, Wojtecki L, Bötzel K, Danek A, Hilker R, Sturm V, Kupsch A, Karner E,
730 Deuschl G (2008) Neuropsychological and psychiatric changes after deep brain
731 stimulation for Parkinson’s disease: a randomised, multicentre study. Lancet Neurol
732 7:605–614.
733 Woolsey CN, Erickson TC, Gilson WE (1979) Localization in somatic sensory and motor areas
734 of human cerebral cortex as determined by direct recording of evoked potentials and
735 electrical stimulation. Journal of Neurosurgery 51:476-506.

736 **FIGURE LEGENDS**

737

738 **Figure 1**. **Experimental paradigm.** ITI = intertrial interval; ISI = interstimulus interval.

739

740 **Figure 2. Location of recording sites in the MNI-defined space.** ***A***, An example trajectory of
741 the DBS lead through the left subthalamic nucleus (STN) shown on the DISTAL atlas by Ewert
742 et al. (2017). ***B***, MNI-defined coordinates (mm) of recording sites in the STN plotted for all
743 subjects in 3D space. ***C***, Reconstructed locations of all ECoG electrodes in the sensorimotor
744 cortex that were included in the study (n = 125), co-registered and plotted on the cortical surface
745 of the MNI brain space. ***D***, MNI-defined coordinates (mm) of the ECoG contacts on the
746 sensorimotor cortex plotted for all subjects in 3D space. In ***B*** and ***D***, each subject's electrodes
747 are mapped with a different color.

748

749 **Figure 3. Subthalamic nucleus (STN) and sensorimotor cortex (SMC) show speech**
750 **production-related time-frequency modulations.** ***A-B***, Grand average of (***A***) STN and (***B***)
751 SMC oscillatory activity (average z-scored spectral power) across all recording sites and all
752 trials aligned to vowel onset (Time = 0 s, grey dashed vertical line). Significant modulations
753 compared to baseline are marked in red contour (Wilcoxon signed-rank, $p < 0.05$, FDR
754 corrected). Average speech production onsets and offsets are marked with grey dotted vertical
755 lines. Rectangles with grey solid lines mark the time window (±500 ms from vowel onset) for the
756 analysis of speech production-related high gamma (60-150 Hz) activity. ***C-D***, Z-scored high
757 gamma (60-150 Hz) power averaged for the 1 s time window (±500 ms from vowel onset)
758 plotted in 3D space for each subject's (***C***) STN and (***D***) SMC recording site. The location of
759 recoding sites is provided in MNI coordinates.

760

761 **Figure 4. Spatial distribution of tongue- and lips-preferred articulatory activity in the MNI-**
762 **defined STN space and sensorimotor cortex (SMC).** ***A*** and ***C***, Outcome of a series of t-tests
763 comparing z-scored high gamma power (averaged for a 500-ms long time window before vowel
764 onset) during articulation of tongue consonants vs. lips consonants for each (***A***) STN and (***C***)
765 SMC recording site. Opacity of the circles varies with the magnitude of the t-value: negative t-
766 values (in blue shades) suggest a greater response to tongue; positive t-values (in red shades)
767 suggest a greater response to lips (Welch two sample t-test, $p < 0.05$). Note that the obtained t-
768 values for the SMC sites differed significantly along the ventral-dorsal and lateral-medial axes
769 (Spearman's rank-order correlation test, $p < 0.01$), suggesting articulator-discriminative
770 somatotopy. Circles with black outline mark representative sites for tongue and lips, whose
771 articulatory activity is plotted on the right. ***B*** and ***D***, Examples of representative tongue-preferred
772 and lips-preferred sites for (***B***) STN and (***D***) SMC. A subtraction time-frequency representation
773 is shown for (***i***) the tongue-preferred site after time-frequency representation for all trials with
774 lips consonants is subtracted from time-frequency representation for all trials with tongue
775 consonants, and for (***iii***) the lips-preferred site after time-frequency representation for all trials
776 with tongue consonants is subtracted from time-frequency representation for all trials with lips
777 consonants. Grey filled contours mark significant time-frequency differences between the two
778 conditions (Wilcoxon rank sum test, $p < 0.05$, FDR corrected). Rectangles with grey solid lines
779 mark the time window (from 0.5 s before vowel onset until vowel onset) for the analysis of
780 articulator-specific high gamma (60-150 Hz) activity. Differences in averaged z-scored high
781 gamma power elicited by trials with the tongue articulation vs. the lips articulation are shown for
782 tongue-specific (***ii***) and lips-specific (***iv***) sites (significant differences are marked with asterisks,
783 Welch two sample t-test, $p < 0.05$). Gray bands mark the time window (from 500 ms before
784 vowel onset until vowel onset) across which high gamma power was averaged for the analysis
785 of articulator-specific activity. Throughout ***i-iv***, grey dashed vertical line represents vowel onset

(Time = 0 s). Dotted vertical lines represent spoken response onsets and offsets for trials with tongue consonants (blue) and trials with lips consonants (red).

Figure 5. Time-course of the articulatory encoding at articulator-discriminative recording sites in the subthalamic nucleus (STN) and sensorimotor cortex (SMC). ***A-B***, Average high gamma activity at the (***A***) STN and (***B***) SMC articulator-responsive recording sites for trials with word-initial tongue (coronal) and word-initial lips (labial) consonants. ***C***, Number of articulator-responsive electrodes in the STN (a total of 23%) and SMC (a total of 30%) broken down by articulator type. ***D***, Distribution of the effect sizes (Hedges' *g*) quantifying the difference in average z-scored high gamma power between trials with word-initial coronal and word-initial labial consonants at each time point of the STN and SMC recordings. Throughout ***A-B***, ***D***, grey dashed vertical lines represent vowel onset (Time = 0 s); dotted vertical lines represent consonant onset.

TABLE LEGENDS

Table 1. Subject demographic and clinical characteristics.

Table 2. Subjects recording and behavioral performance characteristics.

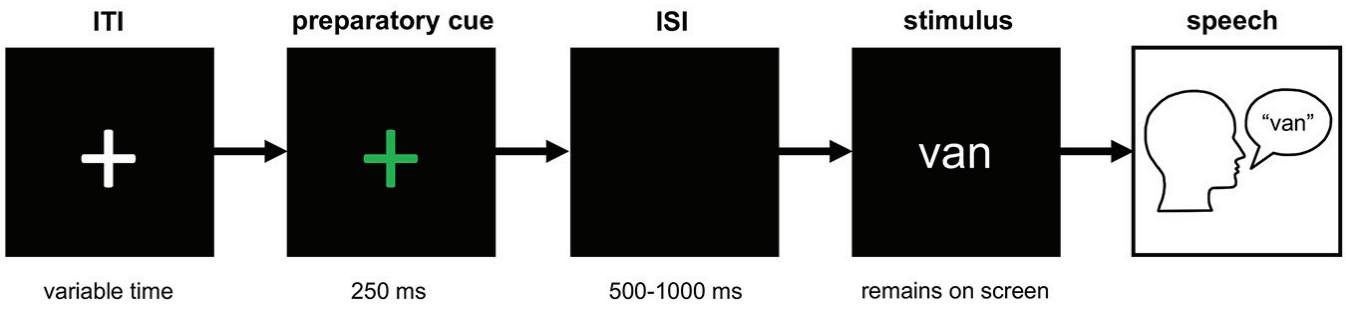

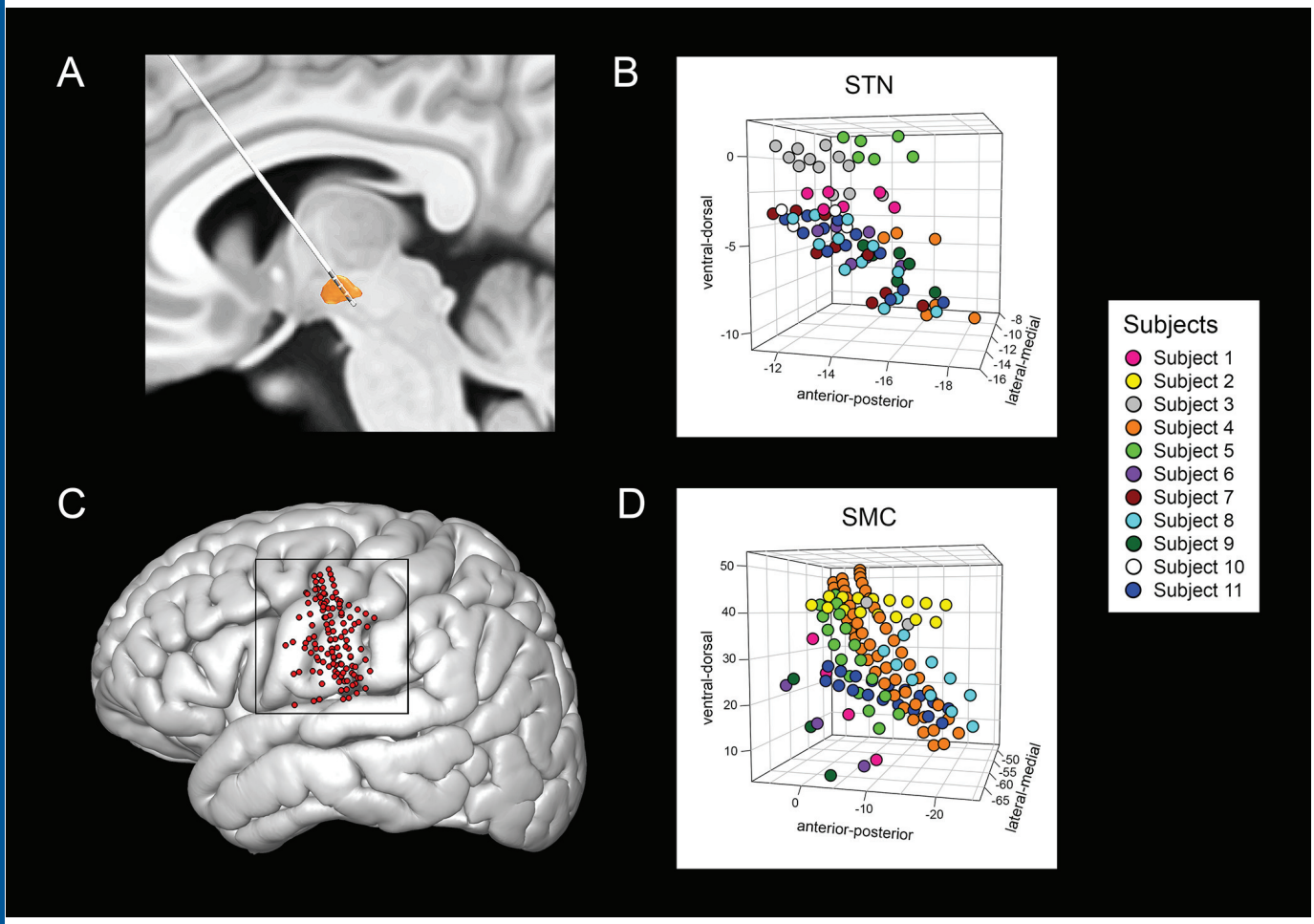

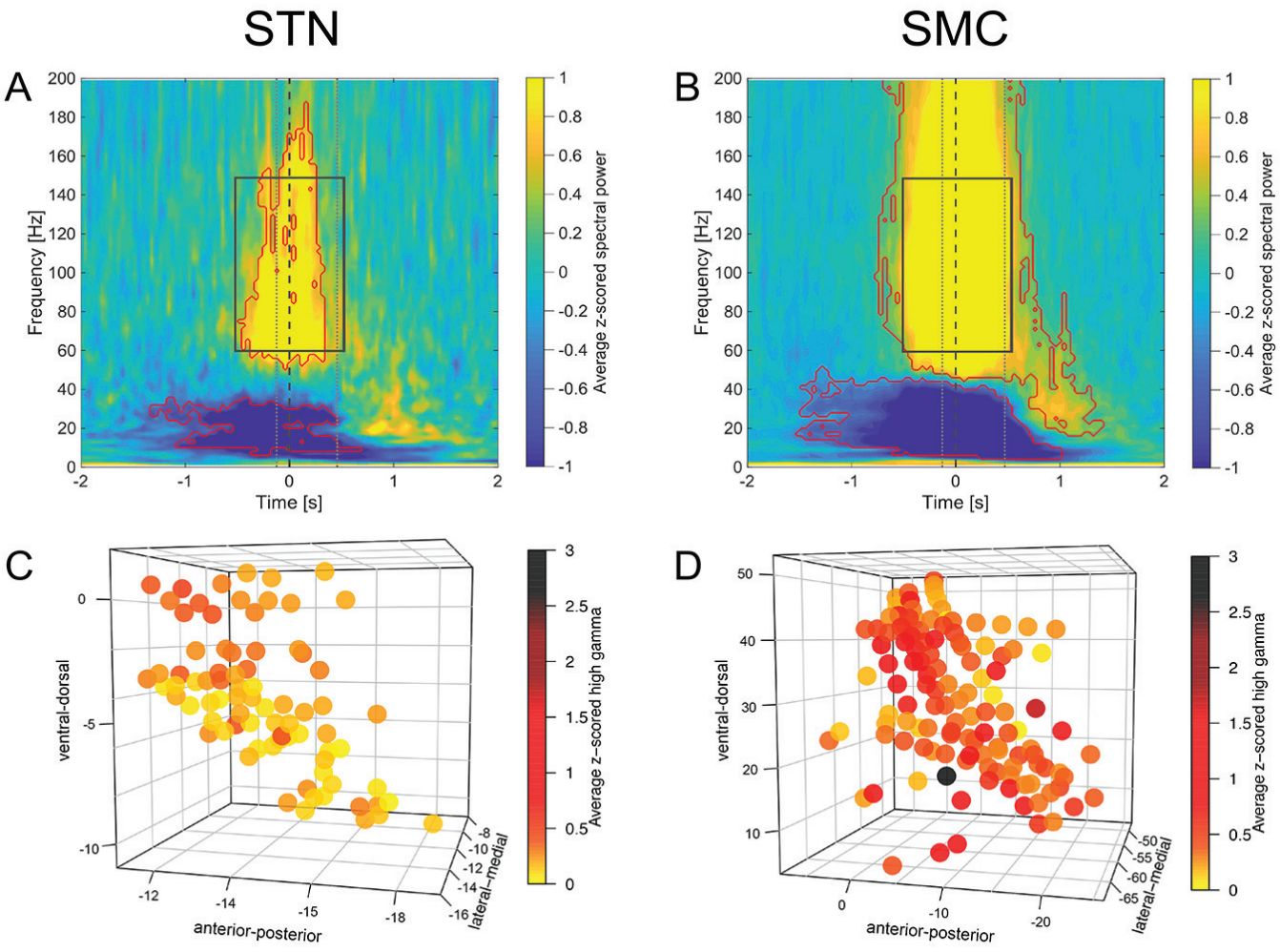

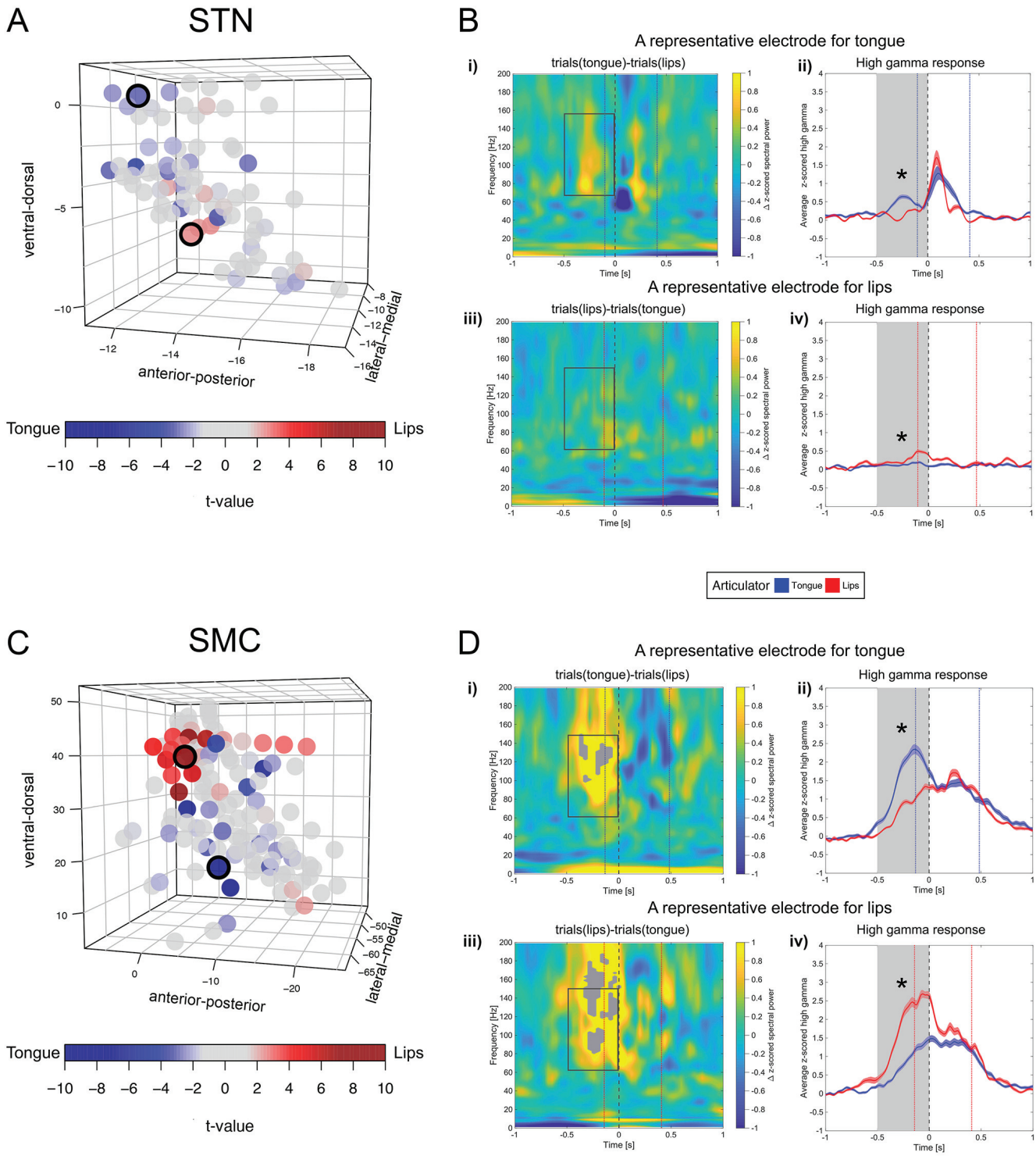

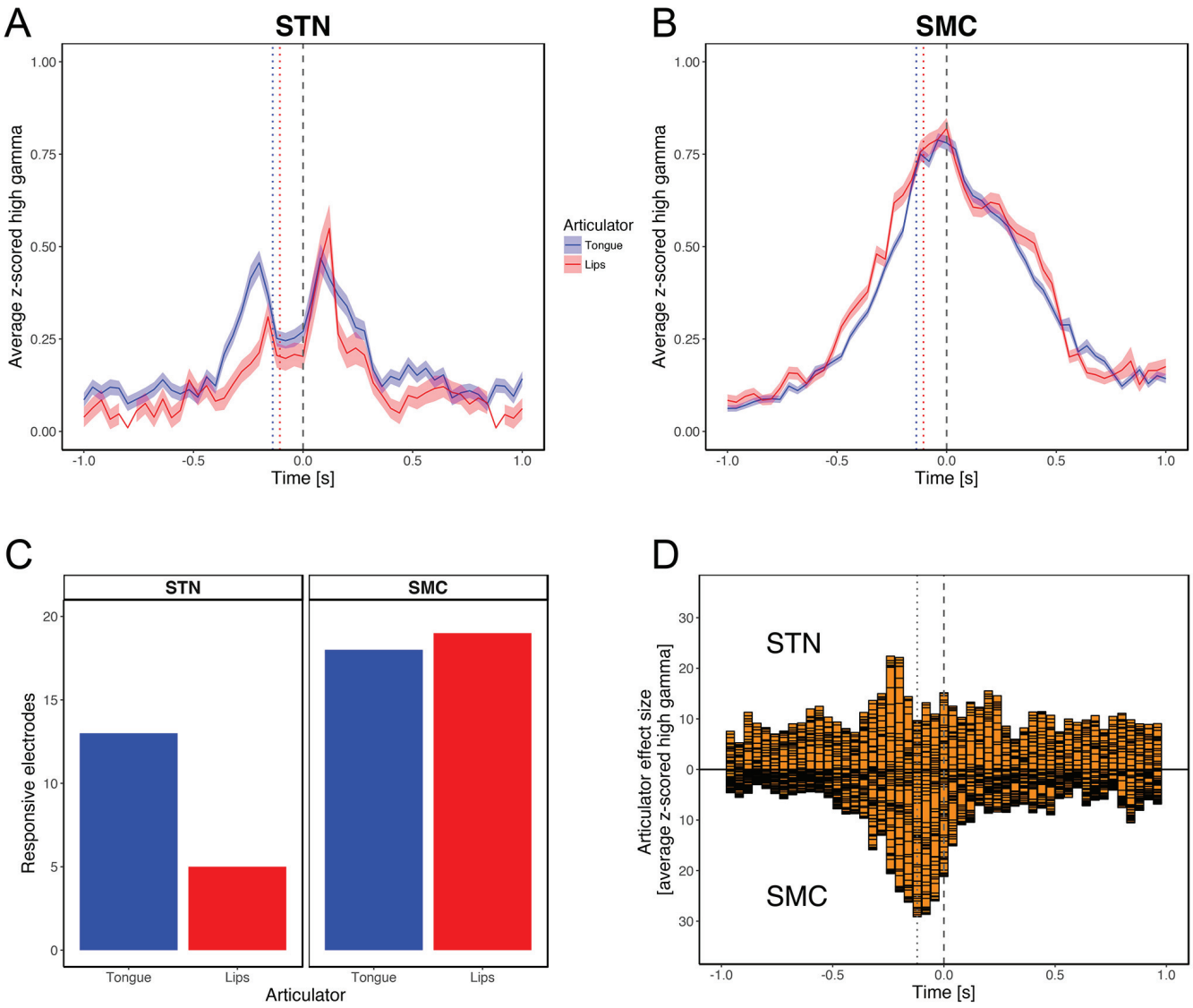

Subject	Gender	Age	Handedness	Education, years	Duration of disease, years	Hoehn and Yahr Stage	UPDRS Score (off medication)
1	Male	71	not recorded	not recorded	6	2	35
2	Male	60	Right	12	14	2	53
3	Male	69	Right	14	9	2	46
4	Male	61	Right	16	5	2	31
5	Male	68	Left	16	8	2	50
6	Male	57	not recorded	not recorded	7	2	44
7	Male	82	Right	16	8	2	36
8	Male	66	Right	19	7	2	45
9	Female	71	Right	16	8	2	24
10	Male	77	Right	18	10	2	27
11	Male	60	Right	13	6	2	39

Subject	Cortical recording	Number of cortical electrode contacts	STN recording	Number of STN electrode contacts	Rejected trials, %	Mean number of included trials per session	Spoken response latency (SD), sec.	Spoken response duration (SD), sec.
1	yes	6	yes	6	34.2	66	1.60 (0.40)	0.59 (0.13)
2	yes	28	not used	not used	20.8	92.5	1.70 (0.60)	0.77 (0.20)
3	yes	6	yes	12	4.5	110	1.18 (0.50)	0.52 (0.09)
4	yes	54	yes	6	4.2	110.5	1.12 (0.38)	0.65 (0.14)
5	yes	28	yes	6	4.6	103.5	0.70 (0.12)	0.62 (0.17)
6	yes	6	yes	6	5	110.5	1.27 (0.43)	0.46 (0.11)
7	not used	not used	yes	9	22.3	59.3	2.62 (1.83)	0.43 (0.08)
8	yes	28	yes	12	2.1	114	0.85 (0.33)	0.63 (0.13)
9	yes	6	yes	6	8.6	91.67	1.12 (0.49)	0.97 (0.36)
10	not used	not used	yes	4	12.7	75.5	1.21 (0.43)	0.54 (0.10)
11	yes	36	yes	12	7.1	105.3	0.99 (0.65)	0.43 (0.11)